JOURNAL OF VIROLOGY, Nov. 2005, p. 14122–14130 Vol. 79, No. 22
0022-538X/05/$08.00+0 doi:10.1128/JVI.79.22.14122–14130.2005

Acquisition of Macrophage Tropism during the Pathogenesis of Feline Infectious Peritonitis Is Determined by Mutations in the Feline Coronavirus Spike Protein

Peter J. M. Rottier,* Kazuya Nakamura,† Pepijn Schellen, Haukeline Volders,‡ and Bert Jan Haijema

Virology Division, Department of Infectious Diseases and Immunology, Faculty of Veterinary Medicine, Utrecht University, Yalelaan 1, 3584 CL Utrecht, The Netherlands

Received 22 June 2005/Accepted 31 August 2005

In feline coronavirus (FCoV) pathogenesis, the ability to infect macrophages is an essential virulence factor. Whereas the low-virulence feline enteric coronavirus (FECV) isolates primarily replicate in the epithelial cells of the enteric tract, highly virulent feline infectious peritonitis virus (FIPV) isolates have acquired the ability to replicate efficiently in macrophages, which allows rapid dissemination of the virulent virus throughout the body. FIPV 79-1146 and FECV 79-1683 are two genetically closely related representatives of the two pathotypes. Whereas FECV 79-1683 causes at the most a mild enteritis in young kittens, FIPV 79-1146 almost invariably induces a lethal peritonitis. The virulence phenotypes correlate with the abilities of these viruses to infect and replicate in macrophages, a feature of FIPV 79-1146 but not of FECV 79-1683. To identify the genetic determinants of the FIPV 79-1146 macrophage tropism, we exchanged regions of its genome with the corresponding parts of FECV 79-1683, after which the ability of the FIPV/FECV hybrid viruses to infect macrophages was tested. Thus, we established that the FIPV spike protein is the determinant for efficient macrophage infection. Interestingly, this property mapped to the C-terminal domain of the protein, implying that the difference in infection efficiency between the two viruses is not determined at the level of receptor usage, which we confirmed by showing that infection by both viruses was equally blocked by antibodies directed against the feline aminopeptidase N receptor. The implications of these findings are discussed.

Viruses interact with their hosts in many different ways, giving rise to infections with highly diverse disease outcomes. Most viral infections can be cleared by the immune system with few adverse effects for the host. Many viruses, however, have evolved active mechanisms for bypassing or disarming host defenses, while in other cases the host immune response, in its attempt to clear the pathogen, causes severe immune-mediated damage. Multiple factors, both host and virus derived, determine the nature and severity of such immune pathology. Well-known examples of viruses that can induce severe immune-mediated damage are dengue, hepatitis C, and respiratory syncytial virus, but it is clear that immune-mediated processes also underlie the pathogenesis of coronaviruses, such as the human severe acute respiratory syndrome (SARS) coronavirus and the feline infectious peritonitis virus (FIPV).

Coronaviruses are a family of enveloped plus-stranded RNA viruses, members of which occur in many animal species as well as in humans, generally causing respiratory or intestinal infections. Coronaviruses of cats, the feline coronaviruses (FCoVs), come in two biotypes. The most common one is the ubiquitous feline enteric coronavirus (FECV) that can cause a mild to moderate transient enteritis in kittens but which may also pass unnoticed. Often, the virus cannot be cleared, and the infection persists in cells of the intestinal mucosa. In contrast, FIPV occurs more sporadically but is highly virulent and induces a usually fatal immunopathological disease characterized by severe systemic inflammatory damage of serosal membranes and disseminated pyogranulomas (for a review, see reference 7). Recent evidence indicates that the two biotypes are merely virulence variants of the same virus and that FIPV actually originates from FECV by mutation within a persistently infected animal (37). The mutation(s) responsible for the virulence transition has not been identified. It appears that no single mutation within any one gene accounts for the shift, though changes in the viral spike gene and in the group-specific genes *3c* and/or *7b* were typically observed (37). Attenuation, on the other hand, is readily observed upon passaging of FIPV in vitro in culture cells, a phenomenon associated with loss-of-function mutations in the *7b* gene (14). Altogether, the results imply a role for several genes, encoding both structural and nonstructural proteins, in virulence.

The transition from FECV to FIPV is accompanied by a remarkable acquisition of macrophage tropism. Whereas FECV replication is primarily restricted to the mature intestinal epithelial cells (27, 28), virulent FIPV strains exhibit a prominent tropism for macrophages (6, 25, 31, 38, 39), infection of which causes a rapid dissemination of the virus throughout the body. FIPV-infected macrophages play a dominant role in bringing about the typical immunopathological damage, as viral antigen can be detected in macrophages in pyogranulomatous lesions in various organs, including liver, spleen, and

* Corresponding author. Mailing address: Virology Division, Faculty of Veterinary Medicine, Utrecht University, P.O. Box 80.165, 3508 TD Utrecht, The Netherlands. Phone: 31-30-2532462. Fax: 31-30-2536723. E-mail: P.Rottier@vet.uu.nl.

† Present address: National Research Center for Protozoan Diseases, Obihiro University of Agriculture and Veterinary Medicine, Obihiro-City, Hokkaido 080-8555, Japan.

‡ Present address: Gynecologic Oncology, University Medical Center Groningen, 9700 RB, Groningen, The Netherlands.

kidney (26). Moreover, severe T-cell depletion, probably as a result of apoptosis (11), has been observed in lymphoid organs in association with FIPV-positive macrophages. The cause of the T-cell depletion is largely unknown, but the release of proinflammatory cytokines with subsequent cytokine dysregulation has been suggested to play a critical role (6, 11). It is of note that the worsening of the respiratory symptoms observed in patients infected with SARS-CoV is also associated with severe immunopathological damage induced by stimulated macrophages (23, 30).

FIPVs efficiently infect and replicate in cultured primary feline peritoneal macrophages, as illustrated by the highly virulent isolate 79-1146. This is in contrast to FECVs, which do so only poorly (35), as exemplified by the genetically closely related but independently obtained FECV isolate 79-1683. FIPV strain 79-1146 was obtained from a 4-day-old kitten that suffered a neonatal death. The lungs, liver, and spleen showed sites of inflammation from which the coronavirus could be isolated (20). The propagated virus was again able to induce a fatal feline infectious peritonitis (FIP) (29). Analysis of strain 79-1146 showed a deletion in the group-specific gene *3c*, a hallmark of FIPV. FECV strain 79-1683 was isolated from an adult cat suffering fatal enteritis, suggested to be panleukemia related. Virus could be detected only in the mesenteric lymph nodes and intestinal wash, indicative of an FECV infection (20). Animal infection with a low-passage cell culture-propagated virus preparation caused an inapparent to mild enteritis (29).

In view of the critical role of macrophages in the pathogenesis of FIP, it seems essential to obtain insight into the molecular basis underlying the acquisition of macrophage tropism during the FECV-to-FIPV conversion. As no pairs of apparently directly related FECV/FIPV isolates have so far been documented, the aim of our present study was to identify the genetic determinants for the macrophage tropism of FIPV 79-1146 by mapping the decisive differences with its close relative FECV 79-1683. To this end, we used our recently developed targeted RNA recombination system (13) to generate a number of chimeric FECV 79-1683/FIPV 79-1146 recombinant viruses which were subsequently tested for their replication in macrophages. Our results demonstrate that the spike gene harbors the sole determinant for efficient macrophage infection. Surprisingly, this property does not reside in the amino-terminal receptor-binding part of the S protein but in the membrane-proximal region of its ectodomain.

MATERIALS AND METHODS

Viruses, cells, and antibodies. *Felis catus* whole fetus (FCWF) cells (American Type Culture Collection) were used to propagate, select, and titrate FIPV strain 79-1146, FECV 79-1683 (20), and recombinant viruses. Mouse LR7 (19) cells were used to propagate mFIPV. Both LR7 and FCWF cells were maintained as monolayer cultures in Dulbecco's modified Eagle's medium containing 10% fetal calf serum (FCS), 100 IU of penicillin/ml, and 100 μg of streptomycin/ml (all from Life Technologies, Ltd., Paisley, United Kingdom). Ascites 9912, derived from an FIPV 79-1146-infected cat, was provided by H. Glansbeek and E. te Lintelo. Hybridoma culture supernatant containing monoclonal antibody (MAb) R-G-4 was kindly provided by T. Hohdatsu (16).

Macrophage isolation, culturing, and infection. In order to isolate bone marrow-derived mononuclear cells (BMMCs), femurs were removed from a clinically healthy, euthanized specific-pathogen-free cat. The femurs were cracked, and the bone marrow was aspirated using phosphate-buffered saline (PBS). The BMMCs were washed twice with PBS and resuspended in Dulbecco's modified Eagle's medium ($2 \cdot 10^7$ cells/ml), after which an equal volume of a 20% dimethyl sulfoxide–80% FCS solution was added. The cells were subsequently frozen and stored at −150°C. In order to culture macrophages, the BMMCs were thawed, washed, and resuspended in Iscove's medium containing 10% FCS, 100 IU of penicillin/ml, and 100 μg of streptomycin/ml (all from Life Technologies, Ltd., Paisley, United Kingdom), after which the cells were incubated in 96-well plates (10^6 cells per well). After 3 days, the nonadherent cells were removed by two washes with prewarmed medium. At day 7, the majority of the adherent BMMCs ($3 \cdot 10^4$ adherent cells per well) had assumed macrophage morphology as characterized by their cytoplasmic vacuoles and their ability to phagocytose dextran. To this end, cells were incubated with fluorescein-labeled dextran in PBS (molecular weight, 70,000 [Molecular Probes]) at a concentration of 100 μg/ml for 30 min at 37°C. Cells were fixed as described below.

To infect the macrophages, the cells were washed with PBS at day 7 postseeding, after which virus, diluted to the appropriate titer in Iscove's medium, was added. At 3 h postinfection (h p.i.), virus was removed by replacing the culture fluid with complete Iscove's medium. The cells were fixed at the indicated time points in 3.7% paraformaldehyde, permeabilized with 70% ethyl alcohol, and washed three times with PBS containing 0.5% fetal bovine serum (FBS). Infected cells were identified immunohistochemically. To block nonspecific antibody binding, the cells were incubated for 30 min at room temperature (RT) in PBS containing 10% FBS, after which they were incubated for 1 h at RT with ascites 9912 diluted 1:500 in PBS containing 5% FBS. The cells were washed three times with PBS containing 5% FBS and incubated for 1 h at RT with goat anti-cat peroxidase (DAKO, Glostrup, Denmark) diluted 1:400 in PBS containing 5% FBS. The cells were then washed three times with PBS and finally stained with 3-amino-9-ethylcarbazole (Brunschwig, Amsterdam, The Netherlands) according to the manufacturer's protocol. As a negative control, mock-infected macrophages were always used to ensure that the anti-FCoV antibodies and anti-cat peroxidase were not nonspecifically staining cells.

Plasmid constructs. Transcription vectors for the production of synthetic donor RNA for targeted recombination were derived from plasmid pBRDI1 (13), which specifies an FIPV 79-1146 RNA transcript consisting of the very 5′ end of the genome (681 nucleotides) fused to the 3′ 363-nucleotide proximal end of ORF1b and running to the 3′ end of the genome (Fig. 1, left). To obtain FECV 79-1683-derived cDNA, genomic viral RNA was extracted from a culture supernatant of cells infected with the virus using a QIAGEN viral RNA kit. First-strand cDNA synthesis (SuperScript II RT, GIBCO-Invitrogen) was performed using a poly(T) primer and the extracted viral RNA as a template. To generate a DNA fragment encompassing the FECV 79-1683 spike gene, a PCR (Expand Long Template PCR system, Roche) was performed using primers 1644 (5′-GGTGAGCTCTGGACTGTGTTTTGTAC-3′) and 311 (5′-CGGTACAAA GCCAAAAATGATAC-3′) and cDNA as a template, resulting in a 5,300-bp fragment. To obtain a DNA fragment containing ORF3abc and the E, M, and N genes of FECV 79-1683, a PCR was performed using primers 1244 (5′-GCC ATTCTCATTGATAAC-3′) and 299 (5′-GATTAAGCAGATGACTGAGTA A-3′) and FECV 79-1683-derived cDNA as a template, resulting in a 3,710-bp fragment. The 5,300-bp DNA fragment containing the entire FECV 79-1683 spike gene was digested with SacI and AflII and ligated into similarly treated pBRDI1, resulting in pBRDI1B (Fig. 1, left). The 3,710-bp fragment containing ORF3abc and the E, M, and N genes of FECV 79-1683 was treated with AflII and Bsu36I and ligated into similarly digested pBRDI1, resulting in pBRDI1C (Fig. 1, left). To construct pBRDI1B3 and pBRDI1B5 (Fig. 1, left), BstEII-AflI and SacI-BstEII fragments of pBRDI1B were isolated and ligated into BstEII-AflI- and SacI-BstEII-treated pBRDI1, respectively. To introduce an out-of-frame deletion into the *7b* gene, a DNA fragment containing this gene construct was amplified by PCR using primer D76 (5′-CTCAATCTAGAGGAAGAC ACC-3′), primer 1249 (5′-GCGGCCGCTTTTTTTTTTTT-3′), and pBRDI1 as a template. The resulting 1,800-bp fragment was cloned into pGEM-T-easy (Promega). This plasmid was digested with BclI, subsequently treated with Klenow, and self-ligated, resulting in the intended out-of-frame mutation in *7b*. The mutated *7b* sequence was isolated from this plasmid by Bsu36I and NotI digestion and introduced into Bsu36I- and NotI-digested pBRDI1, resulting in plasmid pBRDI1A (Fig. 1, left).

To introduce an aspartate-to-alanine substitution at amino acid position 1016 of the FECV 79-1683 spike protein (see Fig. 6B), combinations of primers 1911 (5′-GCAAGTTGAATACATGCAGG-3′) and 1900 (5′-CATTAGCTACCC CGGGTAACAC-3′) and of primers 1898 (5′-GTGTTACCCGGGGTAGCT AATGCTGACAAGATGAC-3′) and 311 (5′-CGGTACAAAGCCAAAAAT GATAC-3′) and FECV 79-1683-derived cDNA as a template were used to generate fragments of 500 bp (fragment A) and 2,000 bp (fragment B), respectively. Fragments A and B were fused using the overlap between both fragments through primers 1898 and 1900 and amplified using primers 1911 and 311,

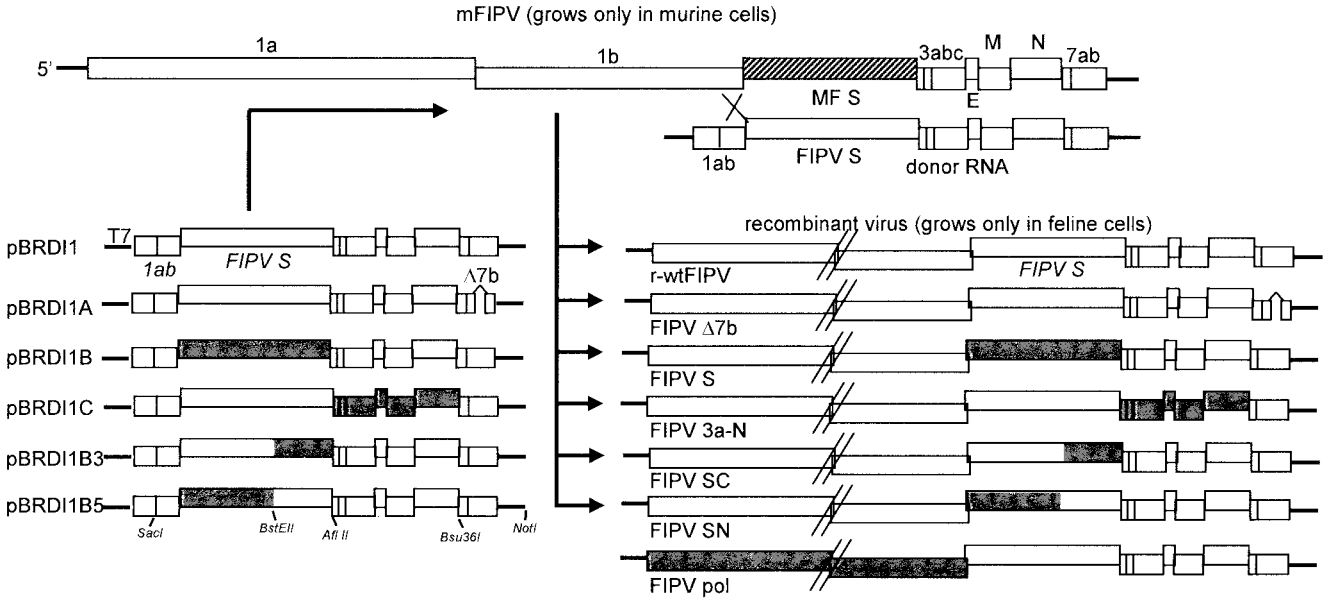

FIG. 1. Construction of recombinant viruses. The transcription vectors from which the synthetic RNAs were made in vitro by using T7 RNA polymerase are indicated at the left. Vector pBRDI1 has been described before (13); the other vectors are derivatives thereof (see Materials and Methods). T7 indicates the position of the T7 promoter; the 1a and 1b boxes represent the in-frame fusion between the 5′-terminal segment of ORF1a and the 3′-terminal domain of ORF1b. The FECV 79-1683-derived sequences are indicated in gray. The scheme at the top pictures the principle of targeted recombination using the interspecies chimeric virus mFIPV, which grows only in murine cells. The region in the mFIPV genome encoding the ectodomain of the MHV S gene is hatched. A single crossover event (indicated by an X) anywhere within the 3′ domain of the ORF1b gene present in donor RNA and viral genome generates a recombinant genome. Recombinant progeny can be selected on the basis of their ability to infect feline cells and their concurrently lost ability to infect murine cells. Recombinant viruses are represented at the right.

resulting in a 2,500-bp fragment (fragment C). Fragment C was digested with BstEII and AflII and ligated into BstEII-AflI-treated pBRDI1B and pBRDI1B3, respectively, resulting in pBRDI1B D>A and pBRDI1B3 D>A.

Targeted RNA recombination. The targeted recombination procedure for constructing the FIPV recombinant viruses was performed as described previously (13). Donor RNA transcripts were synthesized from NotI-linearized pBRDI1, pBRDI1A, pBRDI1B, pBRDI1B3, pBRDI1B5, pBRDI1B D>A, pBRDI1B3 D>A, and pBRDI1C and were each used to transfect LR7 cells that had been infected with mFIPV (Fig. 1). mFIPV encodes a hybrid spike protein (MF S); its ectodomain is derived from mouse hepatitis coronavirus (MHV) S, and the transmembrane domain and cytoplasmic tail are from FIPV S, allowing infection of murine but not feline cells. These cells were then plated on a monolayer of feline FCWF cells. After 48 h of incubation at 37°C, progeny viruses released into the cultured medium were harvested and purified twice by plaque purification on FCWF cells before a passage 1 stock was grown.

To obtain a chimeric recombinant virus of which the entire genomic 5′ part, including ORF1a and ORF1b, was derived from FECV 79-1683 and the remainder from FIPV 79-1146, FCWF cells were first infected with FECV 79-1683 followed by a transfection with donor RNA transcripts synthesized from NotI-linearized pBRDI2 as described previously (13). Plasmid pBRDI2 is identical to pBRDI1 except that it carries the MF S hybrid spike gene. The infected and transfected FCWF cells were then cocultured with murine LR7 cells. To select potential recombinant viruses expressing the MF spike gene and ORF1a and 1b of FECV 79-1683 (designated mFIPV pol), progeny virus released into the cocultured medium was harvested and purified by end-point dilution on LR7 cells before a passage 1 stock was grown. In a second targeted recombination experiment, LR7 cells were infected with mFIPV pol passage 1 followed by a transfection with pBRDI1-derived donor RNA. These cells were then plated on FCWF cells, and potential recombinant viruses (FIPV pol) were isolated as described above.

After confirmation of the recombinant genotypes by reverse transcriptase PCR on purified genomic RNA, passage 2 stocks, which were subsequently used in the experiments, were grown. The passage 2 stocks and the parental viruses FIPV 79-1146 and FECV 79-1683 were titrated on FCWF cells.

RESULTS

Isolation and cultivation of primary bone marrow-derived macrophages. To obtain primary feline bone marrow-derived macrophages for in vitro infection experiments, BMMCs were isolated by lavage from femurs of a specific-pathogen-free cat. The BMMCs were cultured in Iscove's medium for 1 week, after which up to 80% of the adherent cells had assumed the typical morphology of macrophages as characterized by the distinctive presence of cytoplasmic vacuoles (Fig. 2C, panel 1, arrow A) and the ability to phagocytose material (data not shown). Phagocytosis was not observed with nonmacrophage control cells (FCWF cells; data not shown). Besides macrophages, a few fibroblast-like cells were observed (Fig. 2C, panel 1, arrow B).

Infection and replication of FCoVs in bone marrow-derived macrophages. FIPV 79-1146 and FECV 79-1683 have very similar infection and growth properties in FCWF cells. The two viruses infect similar numbers of FCWF cells; typically, when inoculated at a multiplicity of infection (MOI) of 1, approximately 30% of cells are infected when assayed at 6 h p.i. by immunoperoxidase staining (data not shown). In one-step growth experiments, the general shapes of the resulting curves are similar, and both viruses reach almost identical maximal titers in these cells (Fig. 3A).

To determine the infection characteristics of the two viruses in primary bone marrow-derived macrophages, cells (approximately 30,000) were inoculated 1 week postseeding at a MOI of 50. As judged from the shape of the growth curves, the

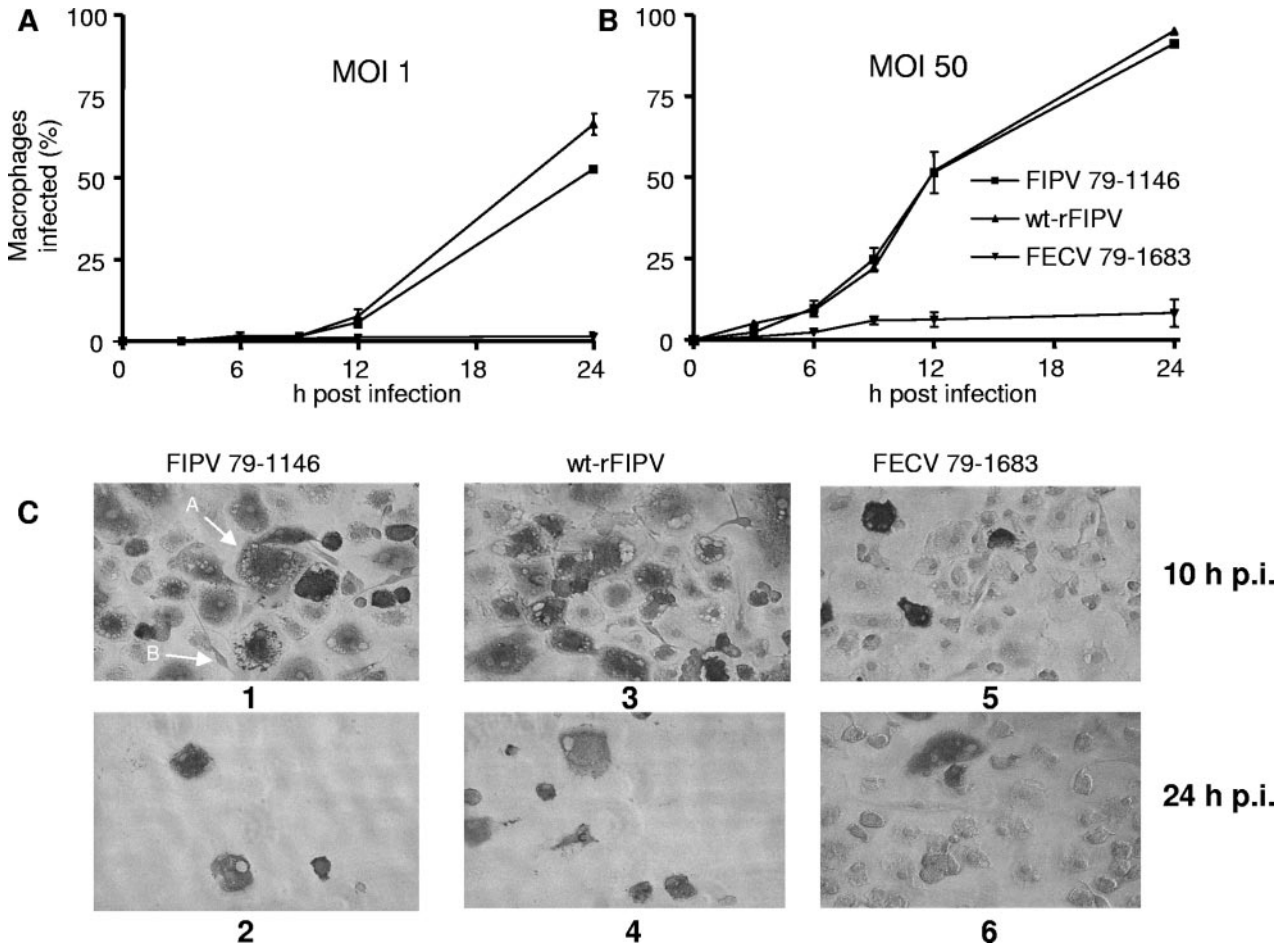

FIG. 2. Infection of primary feline bone marrow-derived macrophages by FIPV 79-1146, FECV 79-1683, and wt-rFIPV (a recombinant copy of wild-type FIPV 79-1146). Inoculations were carried out at low multiplicity (MOI = 1) (A) and high multiplicity (MOI = 50) (B). Data are expressed as the means ± standard errors of three separate experiments. (C) FCoV-infected macrophages (MOI = 50). The cells were stained with antibodies from ascites 9912 at 10 h p.i. and 24 h p.i. Arrows in panel 1 indicate macrophage (A) and fibroblast (B) cells.

multiplication kinetics of the viruses are quite similar, but in contrast to the observations in FCWF cells, the maximal titers reached were always almost 2 log units lower for FECV 79-1683 than for FIPV 79-1146 (Fig. 3B). In these experiments, a wild-type recombinant of FIPV strain 79-1146 (wt-rFIPV) was used as a control. It always behaved indistinguishably from its parental virus (Fig. 2 and 3).

To test whether the observed differences in multiplication are the result of differences in infection efficiency, the susceptibility of macrophages to FCoV infection was investigated. Macrophages were inoculated with each virus both at a low dose (MOI = 1) and at a high dose (MOI = 50). As shown in Fig. 2, FIPV 79-1146 infected the cells quite efficiently. Immunohistochemically, infected macrophages were first detected at 4 to 6 h after inoculation. At the low MOI, approximately 3 to 5% of the cells were FIPV infected when measured at 12 h p.i. (Fig. 2A). These numbers increased sharply with time, as a majority of the cells (up to 60%) appeared to be infected at 24 h p.i. (Fig. 2A), probably as a result of secondary infections. At the high MOI, around 50% of the macrophages were FIPV positive at 12 h p.i. (Fig. 2B), after which the infection gradually eradicated the culture. At 24 h p.i., few cells were left, and the majority of them were infected (Fig. 2B and C, panel 2). In contrast, FECV strain 79-1683 infected the macrophages very poorly. Irrespective of the dose, only low numbers of cells appeared to be infected; when assayed at 12 h p.i., about 1% of the cells inoculated at a MOI of 1 stained positive (Fig. 2A), while 3 to 4% of the cells had become infected at the high MOI (Fig. 2B). Significantly, unlike with FIPV, these numbers hardly increased over time (Fig. 2C, panel 6). Apparently, the virus that is produced by the small number of cells initially infected is unable to spread the infection. The observations illustrate the profound differences in the characteristics of infection of macrophages between FIPV 79-1146 and FECV 79-1683. The results are consistent with observations obtained previously with these viruses using macrophages isolated from the peritoneal cavity (35).

Spike protein determines the ability to infect macrophages. To identify the region(s) in the FCoV genome that determines the efficiency of macrophage infection, a collection of hybrid FIPV/FECV recombinant viruses was constructed by replacing domains of the FIPV 79-1146 genome with the corresponding domains of FECV 79-1683, altogether comprising the complete FCoV genome (Fig. 1) (see Materials and Methods). The

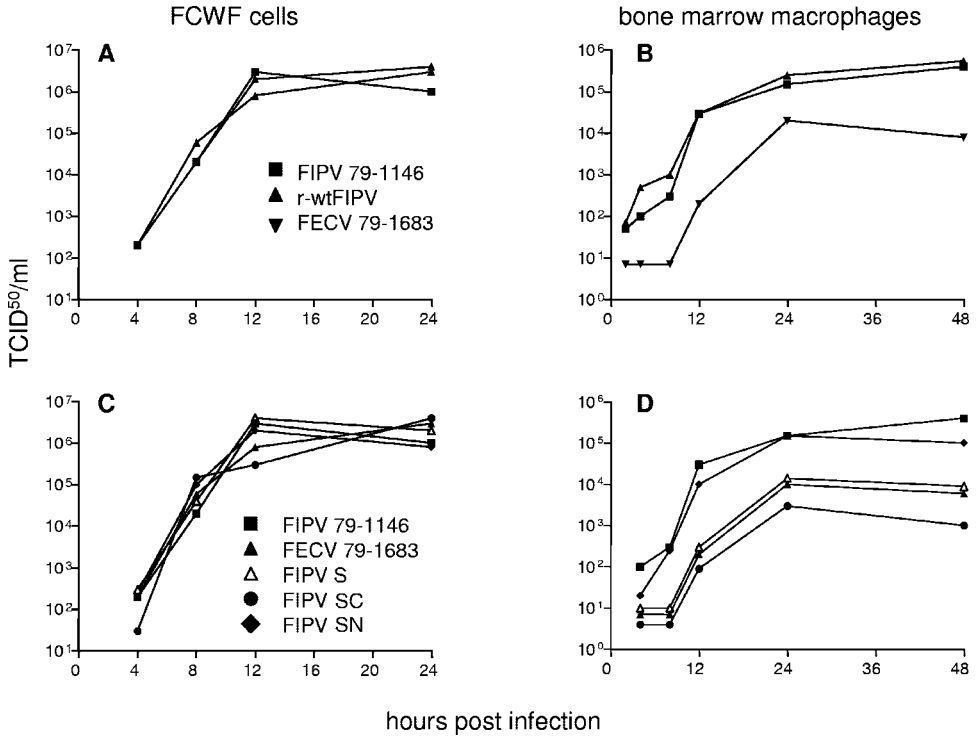

FIG. 3. Growth of FIPV 79-1146, FECV 79-1683, and recombinant viruses in FCWF cells (A and C) and in bone marrow-derived macrophages (B and D). FCWF cells were inoculated at a MOI of 5 and macrophages at a MOI of 50. Viral infectivity in the culture medium was determined at different times postinfection by a quantitative assay using FCWF cells, and 50% tissue culture infective doses ($TCID_{50}$s) were calculated.

recombinant virus designated FIPV pol derives its ORF1a and 1b region from FECV, while the remaining 3′ part of its genome is derived from FIPV. In the recombinant virus named FIPV S, only the S gene is from FECV. In FIPV 3a-N, the genomic segment encompassing ORFs 3a through N has been replaced by that of FECV. The recombinant virus designated FIPV Δ7b contains a loss-of-function deletion in the *7b* gene analogous to the mutation that occurs in the ORF7b region of FECV 79-1683. All recombinant viruses grew well on FCWF cells, showing growth characteristics similar to those of the two parental viruses. Moreover, all recombinant viruses infected approximately similar numbers of FCWF cells (±30% at 6 h p.i.) when inoculated at a MOI of 1 (data not shown).

To assess the ability of the recombinant viruses to infect macrophages, cells were inoculated at a high MOI (50) and fixed for immunostaining at 10 and 24 h p.i.; wt-rFIPV and FECV 79-1683 were used as the controls. As can be observed in Fig. 4A, which shows the situation at 10 h p.i., the recombinant viruses FIPV pol, FIPV 3a-N, and FIPV Δ7b infected bone marrow-derived macrophages as efficiently as the wt-rFIPV control, indicating that ORF1a, 1b, 3abc, and 7b and the E, M, and N genes play no role in the observed macrophage tropism. Consistently, the recombinant viruses lacking the *3abc* (FIPVΔ3abc) or the *7ab* (FIPVΔ7ab) gene clusters, which we described earlier (12), also infect macrophages efficiently (data not shown), demonstrating that the group-specific genes are not required for efficient macrophage infection.

In contrast, the recombinant virus FIPV S exhibited a strongly reduced ability to infect macrophages (2% infected cells at 10 h p.i.), quite similar to the infection efficiency

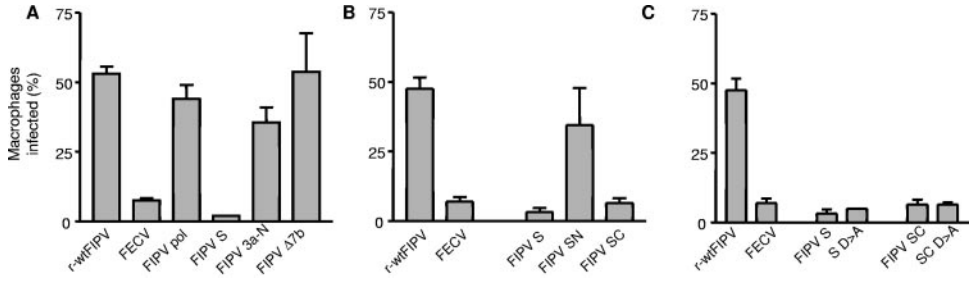

FIG. 4. Comparative infection efficiencies of FCoV (recombinant) viruses in bone marrow-derived macrophages (MOI = 50) expressed as the percentage of infected cells. The cells were immunostained at 10 h p.i. using antibodies from ascites 9912. Data are expressed as the means ± standard errors of results from three separate experiments (A to C).

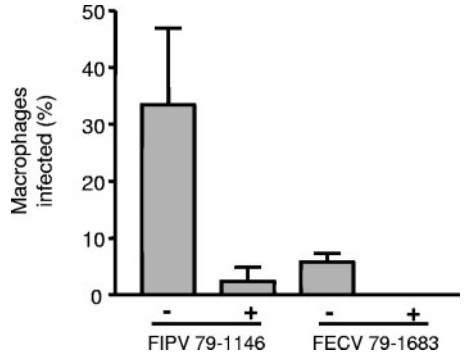

FIG. 5. Inhibition of bone marrow-derived macrophage infection by MAb R-G-4. The cells were infected (MOI = 50) in the presence (+) or absence (−) of MAb R-G-4 (hybridoma culture fluid). Data are expressed as the means ± standard errors of results from three experiments.

observed with FECV 79-1683 (Fig. 4A). Moreover, the number of FIPV S-infected cells in the macrophage culture did not increase with time, again similar to FECV 79-1683 (Fig. 2B and C, panel 6) but unlike the spread of the infection observed at 24 h p.i. with FIPV pol, FIPV 3a-N, FIPV Δ7b, and wt-rFIPV, all of which caused a severe destruction of the macrophage culture (data not shown). Altogether, these results indicate that the macrophage tropism of FCoV is determined solely by its spike protein and suggest that this feature is determined at the level of cell entry.

Both FIPV 79-1146 and FECV 79-1683 use the fAPN receptor to enter macrophages. Both FIPV 79-1146 and FECV 79-1683 use the feline amino peptidase N (fAPN) molecule as a receptor to infect FCWF cells (36). To verify that these viruses also exclusively use this receptor when infecting macrophages, and to exclude the possibility that FIPV 79-1146 but not FECV 79-1683 is able to use a different entry receptor, we inoculated macrophages in the presence of MAb R-G-4. This monoclonal antibody blocks infection of FCWF cells with either virus about 10-fold by its specific binding to the fAPN receptor, as was shown earlier by others (16) and confirmed by us (data not shown). As shown in Fig. 5, the presence of MAb R-G-4 reduced the infection of macrophages by approximately 10-fold, not only with FIPV 79-1146 but as well with FECV 79-1683. These results strongly suggest that the difference in macrophage entry of the viruses is not due to differences at the level of primary receptor usage.

The membrane-proximal region of FIPV 79-1146 spike protein determines macrophage tropism. Coronavirus spike proteins are heavily glycosylated type I membrane proteins with a large ectodomain, a transmembrane anchor, and a small endodomain. In the trimeric spike, the N-terminal regions of the ectodomains form a globular head, while the C-terminal regions occur in a stalklike structure. Biologically, these regions serve different functions: the N-terminal region is involved in receptor recognition, whereas the C-terminal region plays a role in membrane fusion (5). Knowing that primary receptor recognition was not the cause of the differential abilities to infect macrophages, we wanted to further define which domain of the spike protein determines FCoV macrophage tropism. To this end, we generated, in the background of FIPV 79-1146, two isogenic recombinant viruses containing FIPV/FECV chimeric spike genes (Fig. 1). The FIPV SN recombinant encodes a hybrid spike protein whose N-terminal 873 amino acids are derived from FECV and whose remaining C-terminal 582 amino acids are from FIPV. The FIPV SC recombinant, on the other hand, contains the reciprocal hybrid spike gene construct. Both recombinant viruses grew well on FCWF cells and had growth characteristics similar to FIPV 79-1146 (Fig. 3C). When tested on macrophages, the FIPV SN recombinant infected cells efficiently, though to a slightly lower extent than wt-rFIPV (Fig. 4B). At 24 h p.i., most macrophages had been eliminated by the FIPV SN infection, and most of the remaining ones (>90%) were infected (data not shown). In contrast, FIPV SC appeared to infect macrophages only poorly (Fig. 4B), comparable to FECV 79-1683 and FIPV S. Appar-

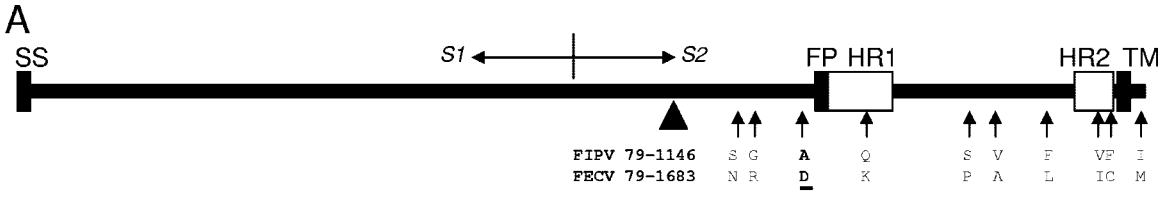

B

```
FECV UCD      (aa 1024-1039) MVLPGVV DDNKMAMYT  |
FECV RM       (aa 1023-1038) MVLPGVV DDNKMAMYT  | serotype I
FIPV UCD 1    (aa 1014-1029) MVLPGVV DGNKMAMYT  |
FIPV UCD 4    (aa 1021-1036) MVLPGVV DANKMSMYT  |
FECV 79-1683 (aa 1008-1023) MVLPGVANDD KMTMYT  | serotype II
FIPV 79-1146 (aa 1006-1021) MVLPGVANAD KMTMYT  |
```

FIG. 6. (A) Schematic representation of the FCoV spike protein structure. The glycoprotein has an N-terminal signal sequence (SS) and a transmembrane domain (TM) close to the C terminus. The C-terminal domain designated S2 contains two putative HR regions (open bars; HR1 and HR2) and the fusion peptide (FP). The fusion point in the hybrid SC and SN spikes is indicated with an arrowhead. Arrows indicate the locations of the 10 amino acid differences between FIPV strain 79-1146 and FECV strain 79-1683. (B) Sequence alignment of the region upstream of the putative fusion peptide from various FCoV strains. The aspartate residues are in bold. The corresponding alanine and glycine substitutions in the FIPV isolates are underlined.

ently, the C-terminal part of the FIPV 79-1146 spike protein defines the macrophage tropism.

We also compared the one-step growth characteristics of the viruses both in macrophages and in FCWF cells. No differences were observed in the fibroblast cultures in either replication kinetics or virus production (Fig. 3C). The viruses also replicated with similar kinetics in macrophages; however, their yields varied significantly (Fig. 3D). The replacement of the FIPV S gene with that of FECV (FIPV S) resulted in significantly reduced virus titers, comparable to those obtained with FECV 79-1683. Of the viruses with a chimeric S gene, FIPV SN grew to similar titers as FIPV 79-1146, whereas FIPV SC replicated to an extent even lower than FECV 79-1683. The results are consistent with the 3′ end of the spike gene being responsible for the efficiency of FCoV growth in macrophages.

Sequence comparison of membrane-proximal regions of FIPV 79-1146 and FECV 79-1683 S protein. A comparison of the C-terminal regions of the FIPV 79-1146 and FECV 79-1683 spike proteins reveals differences in only 10 amino acids (Fig. 6A). These differences are distributed over the entire C-terminal region, including the heptad repeat motifs 1 and 2 (involved in virus-mediated membrane fusion [3]) and the cytoplasmic tail. Closer inspection of these differences to possibly identify the residue(s) critical for the macrophage phenotype revealed that the difference (D>A) located just upstream of the putative fusion peptide occurs in a highly conserved region of the S protein (Fig. 6B). This position has been speculated earlier by Vennema et al. (37) to play a role in the transition of FECV to FIPV after an extensive sequence comparison of avirulent and virulent isolates.

This prompted us to construct FIPV S and FIPV SC derivatives in which a D-to-A substitution was introduced at this position. However, when the growth properties of these recombinant viruses were tested, the viruses appeared to behave as the parental FIPV S and FIPV SC viruses and had not acquired an enhanced macrophage tropism (Fig. 4C). The results indicate that the alanine in the FIPV S protein is not (solely) responsible for the efficient growth in macrophages.

DISCUSSION

Infection of macrophages is a key factor in the pathogenesis of FIP. The emergence of highly pathogenic FIPVs from avirulent enterotropic FECVs is accompanied by a dramatic change in tropism which allows these virulent viruses to infect blood monocytes and, hence, to spread systemically (6, 25, 28, 31, 38, 39). Here we have mapped the mutations that determine this shift in tropism by exchanging genome parts between two related but pathotypically opposite FCoVs. Simply by looking at the fraction of macrophages becoming infected after inoculation with these chimeric viruses, we established that the S gene determines macrophage tropism. This suggested that the difference is made entirely at the level of cell entry. Yet infection by both biotypes remains dependent on interaction with the FCoV receptor fAPN, as shown by the inhibition by a receptor antibody. Consistently, we found that macrophage tropism is determined not by the receptor-binding region of the S protein but by its membrane-proximal domain. The same domain also appeared to determine another interesting difference between the two pathotypes involving the secondary spread of FCoV infection through macrophages. Whereas infection by the avirulent viruses remained restricted to the few cells that had become infected initially, the virulent viruses produced by originally infected macrophages readily infected new cells, leading to the progressive destruction of the entire culture. The results indicate that FCoV infection of macrophages is governed by features of the S protein acting most likely at the level of cell entry rather than at subsequent steps in replication, such as transcription or assembly.

The S protein determines the usually narrow tropism of coronaviruses. It controls all entry functions and provides target cell specificity, as was demonstrated most directly by swapping the spike ectodomains between different coronaviruses and showing their concomitant change in tropism (4, 13, 19). By hindsight, its crucial role in the pathogenesis of FIP through its mediating infection of macrophages should perhaps not have come as a surprise. Accordingly, a number of other examples have shown coronavirus tissue specificity and pathology to be controlled at the level of virus-cell recognition and internalization. When the spike protein of the avian infectious bronchitis virus (IBV) Beaudette strain was replaced by that of the pathogenic M41-CK strain, the recombinant virus (IBV BeauR-M41) acquired the cell tropism of IBV M41-CK in four different cell types (4). However, the introduction of the spike gene of the pathogenic M41-CK strain in a Beaudette background did not result in an increase in pathogenicity, suggesting that the spike gene is not the (sole) determinant for this property (15). A change from a respirotropic to an enterotropic virus was engineered in transmissible gastroenteritis virus by sequence changes exclusively within the transmissible gastroenteritis virus S gene, resulting in a concomitant increase in virulence (1, 33). The mouse hepatitis virus (MHV) S protein has been associated with pathogenicity in several studies. By introducing, for instance, the spike gene of MHV4, a highly neurovirulent strain, into the hepatotropic but mildly neurovirulent MHV-A59, the virus was converted into a neurovirulent variant, demonstrating the role of S in conferring specific virulence features (32).

While the association of the FCoV S protein with macrophage tropism might in retrospect not have been unexpected, the mapping of the functional determinant to the membrane-proximal domain certainly was. The trimeric coronavirus S glycoproteins are type I membrane proteins that form the characteristic spikes protruding from the virion surface. The protein can be divided into several functional domains. The N-terminal region, which constitutes the globular head, is the receptor-binding domain (for a review, see reference 5). The membrane-proximal section of the ectodomain forms a stalklike region and contains two heptad repeat motifs preceded by the putative fusion peptide. These motifs are involved in virus-mediated membrane fusion (3). At the C-terminal end the protein contains a transmembrane domain and a relatively short cytoplasmic tail, both required for incorporation into the virion (2, 10, 40). The localization of the determinant for macrophage tropism in the domain responsible for membrane fusion suggests a role for the fusion function rather than for receptor binding. Though this may seem odd, a correlation between fusion activity and cell tropism and, consequently, virulence has been observed before for coronaviruses. The MHV strain JHM spike protein displays a hyperactive membrane fusion

function (18) that enables JHM viruses to infect tissues with low receptor density, such as mouse neurons, which is probably the cause of its extremely high neurovirulence (9). The hyperactive fusion property of the JHM spike correlates with an unstable interaction between the globular head and the stalk-like region. The reduced stability was hypothesized to lower the free energy required to trigger the conformational change(s) in the spike protein during the membrane fusion process (18). A similar situation might apply for FIPV. Cell culture-adapted MHV-JHM strains, on the other hand, exhibit a more stable S1-S2 interaction and a reduced membrane fusion activity, resulting in limited spread of infection in the central nervous system (9).

Besides the ones in the spike gene, other mutations that have been proposed to be associated with FCoV virulence occur in the group-specific genes *3c* and *7b* (37). Here we show that the group-specific genes of FIPV are not involved in the macrophage tropism. These results corroborate previous results where we showed that viruses lacking the group-specific genes are infectious in the host but do not induce pathology, indicating that these genes contribute to virulence but not at the level of entry (8, 12). Their deletion has no effect on growth in cell culture but converts an otherwise lethal virus into an innocuous derivative. Taken together, these results suggest that the mutational transition from FECV to FIPV is a multistep process, involving (at least) mutations both in the spike gene and in group-specific genes.

In FIPV-infected cats, infected macrophages are abundantly present in all affected lesions. What the role of blood monocytes, the immediate progenitors of the macrophages, is in the pathogenesis of FIP is unclear. Monocyte-associated viremia has also been observed in FCoV-infected healthy cats (17, 21, 34); cell-free virus in blood of such cats has not been detected, probably due to poor replication of FECVs in those cells. Hence, it seems unlikely that the evolution to virulence occurs in these cells. Rather, this process probably occurs in enterocytes, from where the originated FIPV can either gain access directly to the blood and be spread systemically through infected monocytes or first infect regional macrophages in intestinal tissues before entering the bloodstream and infecting monocytes.

FIPV infects macrophages in vitro more efficiently when complexed with S-specific antibodies (using Fc receptor-mediated endocytosis) than on its own (24). Such antibody-dependent enhancement of infection has been observed with a number of human and animal viruses, including influenza viruses, lentiviruses, alphaviruses, and flaviviruses. Interestingly, whereas infection of macrophages by FIPV strain 79-1146 was strongly enhanced by antibodies, infection by FECV strain 79-1683 was not (35). Whether the same region of the spike protein that confers to FIPV its macrophage tropism also determines efficient antibody-dependent enhancement remains to be established.

Feline coronaviruses occur in two serotypes, of which the type I viruses predominate in the field. Serotype II viruses arise by recombination of a type I virus with a canine coronavirus in a doubly infected animal, an event by which the feline virus acquires the S gene (and some flanking sequences) from the canine virus. S proteins of feline and canine coronaviruses share only approximately 45% of amino acid sequences (22) and probably recognize different cell entry receptors. Hence, the recombinant serotype II viruses obtain the fAPN receptor specificity of the donor virus, a feature with great practical consequences because these viruses can be easily grown in vitro, in contrast to the serotype I viruses. Most of our knowledge of the biology of feline coronaviruses is therefore based on studies with serotype II viruses, such as strains 79-1146 and 79-1683, which we used in the present study. It will thus be interesting to find out whether the virulence transition of serotype I viruses involves the same principles, particularly with respect to the acquisition of macrophage tropism.

REFERENCES

1. **Ballesteros, M. L., C. M. Sanchez, and L. Enjuanes.** 1997. Two amino acid changes at the N-terminus of transmissible gastroenteritis coronavirus spike protein result in the loss of enteric tropism. Virology **227:**378–388.
2. **Bosch, B. J., C. A. de Haan, S. L. Smits, and P. J. Rottier.** 2005. Spike protein assembly into the coronavirion: exploring the limits of its sequence requirements. Virology **334:**306–318.
3. **Bosch, B. J., R. van der Zee, C. A. de Haan, and P. J. Rottier.** 2003. The coronavirus spike protein is a class I virus fusion protein: structural and functional characterization of the fusion core complex. J. Virol. **77:** 8801–8811.
4. **Casais, R., B. Dove, D. Cavanagh, and P. Britton.** 2003. Recombinant avian infectious bronchitis virus expressing a heterologous spike gene demonstrates that the spike protein is a determinant of cell tropism. J. Virol. **77:**9084–9089.
5. **Cavanagh, D.** 1995. The coronavirus surface protein, p. 73–103. *In* S. G. Siddell (ed.), The coronaviridae. Plenum Press, New York, N.Y.
6. **Dean, G. A., T. Olivry, C. Stanton, and N. C. Pedersen.** 2003. In vivo cytokine response to experimental feline infectious peritonitis virus infection. Vet. Microbiol. **97:**1–12.
7. **de Groot, R. J. H., and M. C. Horzinek.** 1995. Feline infectious peritonitis, p. 293–309. *In* S. G. Siddell (ed.), The coronaviridae. Plenum Press, New York, N.Y.
8. **de Haan, C. A., P. S. Masters, X. Shen, S. Weiss, and P. J. Rottier.** 2002. The group-specific murine coronavirus genes are not essential, but their deletion, by reverse genetics, is attenuating in the natural host. Virology **296:**177–189.
9. **Gallagher, T. M., and M. J. Buchmeier.** 2001. Coronavirus spike proteins in viral entry and pathogenesis. Virology **279:**371–374.
10. **Godeke, G. J., C. A. de Haan, J. W. Rossen, H. Vennema, and P. J. Rottier.** 2000. Assembly of spikes into coronavirus particles is mediated by the carboxy-terminal domain of the spike protein. J. Virol. **74:**1566–1571.
11. **Haagmans, B. L., H. F. Egberink, and M. C. Horzinek.** 1996. Apoptosis and T-cell depletion during feline infectious peritonitis. J. Virol. **70:**8977–8983.
12. **Haijema, B. J., H. Volders, and P. J. Rottier.** 2004. Live, attenuated coronavirus vaccines through the directed deletion of group-specific genes provide protection against feline infectious peritonitis. J. Virol. **78:**3863–3871.
13. **Haijema, B. J., H. Volders, and P. J. Rottier.** 2003. Switching species tropism: an effective way to manipulate the feline coronavirus genome. J. Virol. **77:**4528–4538.
14. **Herrewegh, A. A., H. Vennema, M. C. Horzinek, P. J. Rottier, and R. J. de Groot.** 1995. The molecular genetics of feline coronaviruses: comparative sequence analysis of the ORF7a/7b transcription unit of different biotypes. Virology **212:**622–631.
15. **Hodgson, T., R. Casais, B. Dove, P. Britton, and D. Cavanagh.** 2004. Recombinant infectious bronchitis coronavirus Beaudette with the spike protein gene of the pathogenic M41 strain remains attenuated but induces protective immunity. J. Virol. **78:**13804–13811.
16. **Hohdatsu, T., Y. Izumiya, Y. Yokoyama, K. Kida, and H. Koyama.** 1998. Differences in virus receptor for type I and type II feline infectious peritonitis virus. Arch. Virol. **143:**839–850.
17. **Kipar, A., S. Bellmann, D. A. Gunn-Moore, W. Leukert, K. Kohler, S. Menger, and M. Reinacher.** 1999. Histopathological alterations of lymphatic tissues in cats without feline infectious peritonitis after long-term exposure to FIP virus. Vet. Microbiol. **69:**131–137.
18. **Krueger, D. K., S. M. Kelly, D. N. Lewicki, R. Ruffolo, and T. M. Gallagher.** 2001. Variations in disparate regions of the murine coronavirus spike protein impact the initiation of membrane fusion. J. Virol. **75:**2792–2802.
19. **Kuo, L., G. J. Godeke, M. J. Raamsman, P. S. Masters, and P. J. Rottier.** 2000. Retargeting of coronavirus by substitution of the spike glycoprotein ectodomain: crossing the host cell species barrier. J. Virol. **74:**1393–1406.
20. **McKeirnan, A. J., J. F. Everman, A. Hargis, L. M. Miller, and R. L. Ott.** 1981. Isolation of feline coronaviruses from two cats with diverse disease manifestations. Feline Prac. **11:**16–20.
21. **Meli, M., A. Kipar, C. Muller, K. Jenal, E. Gonczi, N. Borel, D. Gunn-Moore, S. Chalmers, F. Lin, M. Reinacher, and H. Lutz.** 2004. High viral loads despite absence of clinical and pathological findings in cats experimentally

infected with feline coronavirus (FCoV) type I and in naturally FCoV-infected cats. J. Feline Med. Surg. **6:**69–81.
22. **Motokawa, K., T. Hohdatsu, H. Hashimoto, and H. Koyama.** 1996. Comparison of the amino acid sequence and phylogenetic analysis of the peplomer, integral membrane and nucleocapsid proteins of feline, canine and porcine coronaviruses. Microbiol. Immunol. **40:**425–433.
23. **Nicholls, J. M., L. L. Poon, K. C. Lee, W. F. Ng, S. T. Lai, C. Y. Leung, C. M. Chu, P. K. Hui, K. L. Mak, W. Lim, K. W. Yan, K. H. Chan, N. C. Tsang, Y. Guan, K. Y. Yuen, and J. S. Peiris.** 2003. Lung pathology of fatal severe acute respiratory syndrome. Lancet **361:**1773–1778.
24. **Olsen, C. W., W. V. Corapi, C. K. Ngichabe, J. D. Baines, and F. W. Scott.** 1992. Monoclonal antibodies to the spike protein of feline infectious peritonitis virus mediate antibody-dependent enhancement of infection of feline macrophages. J. Virol. **66:**956–965.
25. **Pedersen, N. C.** 1976. Morphologic and physical characteristics of feline infectious peritonitis virus and its growth in autochthonous peritoneal cell cultures. Am. J. Vet. Res. **37:**567–572.
26. **Pedersen, N. C.** 1987. Virologic and immunologic aspects of feline infectious peritonitis virus infection. Adv. Exp. Med. Biol. **218:**529–550.
27. **Pedersen, N. C., J. W. Black, J. F. Boyle, J. F. Evermann, A. J. McKeirnan, and R. L. Ott.** 1984. Pathogenic differences between various feline coronavirus isolates. Adv. Exp. Med. Biol. **173:**365–380.
28. **Pedersen, N. C., J. F. Boyle, K. Floyd, A. Fudge, and J. Barker.** 1981. An enteric coronavirus infection of cats and its relationship to feline infectious peritonitis. Am. J. Vet. Res. **42:**368–377.
29. **Pedersen, N. C., J. F. Evermann, A. J. McKeirnan, and R. L. Ott.** 1984. Pathogenicity studies of feline coronavirus isolates 79-1146 and 79-1683. Am. J. Vet. Res. **45:**2580–2585.
30. **Peiris, J. S., C. M. Chu, V. C. Cheng, K. S. Chan, I. F. Hung, L. L. Poon, K. I. Law, B. S. Tang, T. Y. Hon, C. S. Chan, K. H. Chan, J. S. Ng, B. J. Zheng, W. L. Ng, R. W. Lai, Y. Guan, and K. Y. Yuen.** 2003. Clinical progression and viral load in a community outbreak of coronavirus-associated SARS pneumonia: a prospective study. Lancet **361:**1767–1772.
31. **Petersen, N. C., and J. F. Boyle.** 1980. Immunologic phenomena in the effusive form of feline infectious peritonitis. Am. J. Vet. Res. **41:**868–876.
32. **Phillips, J. J., M. M. Chua, E. Lavi, and S. R. Weiss.** 1999. Pathogenesis of chimeric MHV4/MHV-A59 recombinant viruses: the murine coronavirus spike protein is a major determinant of neurovirulence. J. Virol. **73:**7752–7760.
33. **Sanchez, C. M., A. Izeta, J. M. Sanchez-Morgado, S. Alonso, I. Sola, M. Balasch, J. Plana-Duran, and L. Enjuanes.** 1999. Targeted recombination demonstrates that the spike gene of transmissible gastroenteritis coronavirus is a determinant of its enteric tropism and virulence. J. Virol. **73:**7607–7618.
34. **Simons, F. A., H. Vennema, J. E. Rofina, J. M. Pol, M. C. Horzinek, P. J. Rottier, and H. F. Egberink.** 2005. A mRNA PCR for the diagnosis of feline infectious peritonitis. J. Virol. Methods **124:**111–116.
35. **Stoddart, C. A., and F. W. Scott.** 1989. Intrinsic resistance of feline peritoneal macrophages to coronavirus infection correlates with in vivo virulence. J. Virol. **63:**436–440.
36. **Tresnan, D. B., R. Levis, and K. V. Holmes.** 1996. Feline aminopeptidase N serves as a receptor for feline, canine, porcine, and human coronaviruses in serogroup I. J. Virol. **70:**8669–8674.
37. **Vennema, H., A. Poland, J. Foley, and N. C. Pedersen.** 1998. Feline infectious peritonitis viruses arise by mutation from endemic feline enteric coronaviruses. Virology **243:**150–157.
38. **Ward, J. M.** 1970. Morphogenesis of a virus in cats with experimental feline infectious peritonitis. Virology **41:**191–194.
39. **Weiss, R. C., and F. W. Scott.** 1981. Pathogenesis of feline infectious peritonitis: pathologic changes and immunofluorescence. Am. J. Vet. Res. **42:**2036–2048.
40. **Ye, R., C. Montalto-Morrison, and P. S. Masters.** 2004. Genetic analysis of determinants for spike glycoprotein assembly into murine coronavirus virions: distinct roles for charge-rich and cysteine-rich regions of the endodomain. J. Virol. **78:**9904–9917.